Compositional analysis of high throughput sequencing data

Greg Gloor

26 January, 2018

Contents

Introduction

About this document

This document is an .Rmd document and can be found at:

github.com/ggloor/templates

The document is a template for two column R markdown. It requires an installation of LaTeXto work properly. This document contains interspersed markdown and R code that may be compiled into a pdf document and supports the figures and assertions in the main article. R code is exposed in the pdf document so that the interested reader can work through the example code themselves.

Reproducing the analysis

From an R command prompt you can compile this document into PDF if you have LaTeXand pandoc installed:

`rmarkdown::render('two_column.Rmd')` or you can open the file in RStudio and compile in that environment.

R packages required

We will need the following R packages, several functions are defined in a dedicated functions section.

1. knitr (CRAN)

This booklet is intended for use in teaching graduate student courses and conference workshops on using compositional data analysis methods to examine high throughput sequencing datasets. The approach taken here is largely intuitive and hands on. Formulas for basic methodologies are presented, but the intuitive reason for using them takes precedence. The methods presented here have been used for 16S rRNA gene sequencing, transcriptomics, metagenomics and in-vitro selection (selex) experiments.

I begin with background and theory, and progress to practical examples. I hope you find this useful.

Outline of the material

- I begin with a brief overview of sequencing technologies, and describe how and why these instruments generate data that are constrained to a constant count.
- I next semi-formally introduce compositional data, and describe with examples the pathologies associated with this type of data.
- I then introduce common data transforms and distances used in the high throughput sequencing literature, and demonstrate that none of the transforms affects the compositional nature of the data, and that in fact, many of the transforms affect the data in non-intuitive ways
- I then introduce sequencing as a stochastic process, explain why we need to estimate our technical variance and show how this can be done technical variance
- I begin the practical part with exploratory data analysis using the compositional biplot
- I describe the properties of three types of plots to examine high dimensional data: Bland-Altman plots (MA plots), volcano plots, and effect plots
- I describe compositionally appropriate methods to estimate differential abundance with an emphasis on ALDEx2 and to a lesser extent ANCOM
- I describe compositional association as a replacement for correlation using the propr R package

The nature of sequencing data

The human microbiome project has initiated the large-scale culture-independent analysis of microbial communities, and transcriptome analysis has led to the study of the transcriptional response to many different disease and ecological states.

However, many studies fail to replicate earlier studies even when the same technologies and strategies are used. As just one example, a multitude of studies have examined the link between autism and the human gut microbiota. These have variously implicated x,y,. . . ,and z microbe as being linked to the condition. In a recent high-profile paper by Hsiao et al. (2013), *Bacillus fragilis* was suggested to restore the gut microbiome of a mouse autism model from 'autistic-like' to 'normal'. Examination of the dataset shows that the conclusion was likely due to chance alone (Gloor and Reid, 2016; Gloor et al., 2016b). While the autism dataset serves as a facile example, the literature are replete with other examples.

DNA sequencing describes a random sample of the environment

All high throughput gene sequencing datasets share a common origin and it is important to understand the source of the data, and the standard workflow. In the first step, an arbitrarily large population of DNA molecules is randomly sampled from an environment. The random sampling can be direct, in the case of genomics or metagenomics DNA is made directly from the sample. Sampling can be indiredt in the case of RNA-seq where RNA molecules are sampled after they have been converted to DNA via reverse transcription. Regardless, the DNA molecules are typically fragmented. Sampling can also be indirect in the case of tag-sequencing or single cell sequencing. In tag-sequencing, most typically applied to 16S rRNA gene sequencing, a small defined region is amplified by the PCR. In single cell sequencing the molecules from a single cell are fragmented and amplified.

In the second step, an aliquot of the population of DNA fragments are used to make a library by attaching standard sequences that permit the DNA fragments to be bound to the solid phase sequencing chip particular to a particular platform.

In the third step a sample of the library is loaded onto a sequencing platform. It is important to understand that all sequencing platforms in widespread use contain a fixed number of locations to which the DNA fragments can bind.

This standardized workflow can be thought of as three random samples from an urn containing a random assortment of DNA fragments. The first random sample is the sample from the environment itself that is used to make the DNA: what is swabbed, and how much is collected relative to the environment. Depending on the environment, the subset of molecules sampled can be a large and complete sample or a small, incomplete and unrepresentative sample. The second random sample is the subset of DNA fragments that are input into the library preparation reaction. Here, the number of fragments available depends on the initial amount of the DNA, the mean fragment size and the requirements of the library preparation protocol. However, all library preparation protocols required more DNA fragments than can be loaded onto the instrument, an example calculation is given below. The third random sample comprise the subset of DNA fragments from the library that are actually sequenced on the machine.

Instrument capacity

The Ion Torrent and Ion Proton systems have a chip with a predetermined number of pores on the sequencing chip (10 of thousands to 10s of millions, depending on the chip) that can accept a library fragment. No signal is returned from an empty pore, and the signal is rejected if a pore contains two or more different fragments. Sequencing is successful only when the pore is occupied by a single fragment from the library.

The Illumina sequencing instruments attach the DNA fragments to a glass slide and then each fragment is amplified into millions of identical fragments called clusters, which appear as randomly distributed spots under a microscope. Each different Illumina instrument accommodates a characteristic maximum number of clusters, and if two or more clusters overlap they are rejected by the software.

Thus, regardless of instrument, the technician must apply a precise number of DNA molecules that maximizes the number of fragments on the sequencing instrument without overloading it. It should be obvious that loading a DNA sequencer is akin to filling the squares on a checkerboard where the goal is to have as many checkers as possible, without overlapping the pieces.

Example calculation of fragment number

The number of fragments after sequencing is determined by the instrument; an Ilumina MiSeq delivers $\sim$ 20M fragments whereas an Illumina NextSeq delivers $\sim$ 400M and an Illumina HiSeq can deliver $\sim$ 250M reads per lane on each of 8 lanes. The commonly used Nextera DNA library kit is optimized to require 50 ng of DNA per sample. Thus, the number of fragments of DNA (or RNA) molecules in the underlying environment, in general, vastly outnumbers the number of sequence fragments from which the library is made, and the number of

fragments in the library in turn outnumbers the number of fragments from which sequencing data are ultimately derived. We can do a simple back of the envelope calculation for an example metagenomics sequencing run to show this.

Assume that we have a mixture of bacterial species with a mean genome size of 4 Mb. One mole of genomes would have a mass of 2.64×10^9 grams. A typical bacterial density for a metagenome would be on the order of at least 10^7 bacteria per ml of sample, so if we take a 1 ml sample, this is 10^7 genomes, which corresponds to about 44 ng of DNA.

If the DNA concentration after isolation is 1 ng/μl, and one μl of DNA is taken, this corresponds to $(1 \times 10^{-9}\text{ g})/(2.64 \times 10^9\text{ g/mole}) \times (6.02 \times 10^{23}\text{ genomes/mole}) = 228,000$ genomes. The Illumina Nextera XT kit can be used to make a library with this amount of DNA. Recall that the the DNA is fragmented, typically into 500 bp or smaller sizes. Using a fragment size of 500 bp, this corresponds to approximately 1.8×10^9 DNA fragments.

In the scenario where a single sample is prepared and run only 1% of DNA fragments in the library will be sequenced on the Illumina MiSeq, and only 22% of the DNA fragmments will be sequenced on the Illumina NextSeq. DNA sequencing rarely involves a single sample, but instead samples are 'multiplexed' on the sequencing run by mixing two or more libraries together. When this occurs the samples have a unique tag, or barcode, attached so that the samples can be uniquely identified post sequencing (Andersson et al., 2008; Gloor et al., 2010; Parameswaran et al., 2007). Barcodes can be added by ligation or by incorporation into PCR primers that are used to amplify the library. Obviously, increasing the number of samples through multiplexing will result in an even smaller proportion of the fragments in each library being sequenced.

DNA sequencing is not counting

From the above, it should be clear that DNA sequencing is not a counting operation but is instead a random sampling operation from a large pool, akin to sampling different colored balls from an urn containing more balls than are sampled. A counting operation always allows the addition of 'one more observation'. In the context of DNA sequencing this would equate to loading the samples onto an Illumina MiSeq chip to the optimal fragment density and then adding in 'one more fragment' repeatedly until the number of fragments loaded exceed the capacity of the chip. The sequencing reaction will fail when the number of frangments exceeds the chip capacity. Stated bluntly, one cannot purchase an Illumina MiSeq run and expect to receive data equivalent to an Illumina NextSeq or HiSeq run. This self-evident fact is completely overlooked in the literature.

If the number of DNA fragments sequenced is has an arbitrary upper bound determined by the machine, and the number of fragments in the library is always larger than the machine capacity, then it should be obvious that the number of fragments sequenced can contain no information about the *number* of fragments in the library pool, nor can the number of fragments contain information about the *number* of molecules in the original DNA sample from the environment. The univariate logical equivalent is to only know the percentage that a suit is marked down to, without knowing the original price. The multivariate intuition is that we cannot know the number of balls of different colour in the urn, we can only infer their proportions.

Therefore, the only information available is the *relative* proportion of individual fragments in the library, which is assumed to approximate the proportion of fragments in the DNA sample from the environment.We will revisit this issue when we discuss normalizations in common use.

Random processes in sequencing

The random sampling process in DNA sequencing has at least three overlapping stochastic processes; environmental sampling, fragment sampling and multiplex sampling.

Sampling from the environment is random since the investigator never collects all the DNA samples from an environment, but rather collects a small aliquot from a specific time or place in the environment. Only the DNA molecules actually collected are used to make the DNA library, and these molecules are assumed to be representative of the environment. Note that this assumption may not always be true. For example, it has been observed that different microbial compositions are observed when collecting stool samples if a sample is taken from the interior or exterior of the stool (Gorzelak et al., 2015).

Fragment sampling occurs because as noted above the fragments actually sequenced are a random sample of the fragments that are in the sequencing library. There are always more fragments in the library than can be accommodated on the instrument, and there are almost always more molecules in the environment than can be accommodated in the library. The sole exception to this rule would be when sequencing is used to investigate low biomass environments—however in this case the library protocols always have an amplification step that increases the number of fragments above the number that can be accommodated on the instrument. The fragment sampling occurs by a multivariate Poisson process (Fernandes et al., 2013).

Two or more independent libraries are mixed together into a multiplex library, and this adds a third level of randomness into the process. The number of fragments in each library is one of the strongest influences on the apparent information in the sample (Horner-Devine et al., 2004; Weiss et al., 2017). The number of fragments observed post sequencing is termed the `library size' or the ''depth of coverage'. In other words, the number of fragments identified in a sample post sequencing is a confounding variable.

The apparent solution to the sequencing depth problem is to normalize the read count values across samples in some way. One method of normalization to is by subsampling, often termed rarefaction, as this is observed to reduce the influence of sequencing depth on variation in α and β diversity metrics (Horner-Devine et al., 2004; Weiss et al., 2017). Another is to convert the data to proportions or percentages; these latter values are widely spoken of in the literature as 'relative abundances'. Subsampling is frequently used to estimate the associated sampling error. Some groups have begun advocating the use of normalization methods prevalent in the RNA-seq field(McMurdie and Holmes, 2014) but still treat the data as point estimates of the true abundance. There are many other normalizations that are used in the ecological and high throughput sequencing literature and the purpose and effect of these on simulated data are explored in the section on Data Transformations.

Sequencing post processing

After sequencing fragments are grouped in some way

Mapping

Fragments generated from metagenomic or RNA-seq experiments are aligned to reference sequences corresponding to genes, transcripts or genetic intervals (generically genes). The total number of fragments mapping to a given gene is said to be the read count for that gene and the read count for all genes in a system ranges from 0 (no fragments align to that gene) to the total number of fragments in the sample. The output from these types of experiments is a table of read counts per gene per sample.

Expand this to outline methods

OTU generation

Fragments generated from tag-sequencing are often merged into operational taxonomic units (OTUs) at some predefined percent identity, or tabulated by the number of identical fragments observed (ASUs). The output from these types of experiments is a table of counts per OTU per sample.

DNA sequencing data are compositions

High throughput sequencing generates compositional data

In the previous chapter we saw that the capacity of the sequencing instrument imposed an upper bound on the total number of fragments that could be obtained from a given sequencing run. We also saw that the process of sequencing is essentially a random sampling of an environment where the environment contains more fragments than can possibly be sequenced. Finally, the data obtained are read counts per genetic interval (gene or OTU) per sample.

The read counts per sample range from 0 to, as a maximum, the total number of reads in the sample. Thus the data are positive integer data with an arbitrary maximum. While the data have an arbitrary maximum, the majority of current tools assume the data are counts and ignore the arbitrary maximum constraint. This assumption is the basis of methods grounded in distributions such as the zero inflated Gaussian (ZIG) (Paulson et al., 2013), negative binomial (Robinson et al., 2010) and Poisson based models (Auer and Doerge, 2011). Recent benchmarking has demonstrated that such methods are unpredictable when dealing with highly sparse data (Thorsen et al., 2016) and do not control the false discovery rate (Gloor et al., 2016a; Hawinkel et al., 2017).

Data of this type are called count compositions, and a number of groups have started to work on developing appropriate methods to deal with high throughput datasets as count compostions (Egozcue et al., 2018; Erb and Notredame, 2016; Erb et al., 2017; Fernandes et al., 2013, 2014; Friedman and Alm, 2012; Gloor and Reid, 2016; Gloor et al., 2016b; Kaul et al., 2017; Kurtz et al., 2015; Lovell et al., 2015; Mandal et al., 2015; Quinn et al., 2017a, 2017b; Silverman et al., 2017; Tsilimigras and Fodor, 2016; Washburne et al., 2017).

So what is compositional data, and what are its properties with respect to high throughput sequencing that make this an important issue?

Compositional data

Data from high throughput sequencing have the following properties; the data are counts, the data are non-negative, and the data has an upper bound imposed by the instrument because there is a limit to the number of fragments (and hence gene or OTU counts) that can be observed. This fits with the definition of compositional data: the data contains D features (OTUs, genes, etc), where the count of each feature is non-negative, and the sum of the parts is known (Aitchison, 1986, pg25). Note that the data do not have to sum to a predetermined amount, it is sufficient that the sum of the parts be known and not be able to be exceeded.

A vector containing D features where the sum is 1 can be formally stated as: $\vec{X} = \{(x_1, x_2, x_3, \ldots x_D); x_i \geq 0; \sum_{x=1}^{D} = 1\}$. The sum of the parts is usually set to 1 or 100, but can take any value; i.e., any composition can be scaled to any arbitrary sum such as a ppm. The property of scaling to any arbitrary value is named an equivalence class and compositional data are equivalence classes (Barceló-Vidal et al., 2001). In the lexicon of high throughput sequencing the vector is the sample and the features are the OTUs or genes or genomic intervals. The total sum is the total number of fragments observed for the sample.

Compositional data have a number of built-in pathologies: a negative correlation bias, sub-compositional incoherence, and spurious correlations. A proper analysis of compositional data must account for these pathologies, and in addition be scale invariant, permutation invariant, and exhibit subcompositional coherence (or at least sub-compositional dominance).

More formally, compositional datasets have the property that they are described by $D-1$ observations (Aitchison, 1986). In other words, if we know that all parts sum to 1, then the last part can be known by subtracting the sum of all other parts from 1, i.e., $x_D = 1 - \sum_{x=1}^{D-1}$. Graphically, this means that compositions inhabit a space called a Simplex that contains 1 fewer dimensions than the number of parts. The distances between parts on the Simplex are not linear. This is important because all parametric statistical tests assume that differences between parts are linear (or additive). Thus, while standard tests will produce output, the output will be misleading because distances on the simplex are non-linear and bounded (Martín-Fernández et al., 1998). The chapter on Data Transformations contains an intuitive demonstration of how data is moved to the Simplex.

Negative correlation bias in compositions

The values of the parts of compositional datasets are constrained because of the constant sum, and this constraint has been known for a very long time. The features in a composition have a negative correlation bias since an increase in the value of one part must be offset by a decrease in value of one or more other parts. In the illustration above, we see that 'V' and 'M' are perfectly

balanced on the fulcrum because they have the same mass. If M becomes heavier, then V will rise even though the mass of V has not changed. The same principle operates in compositional data. If V is the amount of money spend on vegetables, and M is the amount of money spent on meat, and the total food budget is a constant, then the only way that more meat would be consumed would be to spend less on vegetables. Therefore, the amount of money spent on V and M will be perfectly negatively correlated if the total food budget is constrained. This example generalizes to any number of items in the shopping basket as long as the total budget is constrained. When there are more items, then an increase in one item (say shoes) must be offset by a decrease in another item, but it could be a decrease in meat, vegetables or both.

Spurious correlations:

In addition to a negative correlation bias, compositional data has the additional problem of spurious correlation (Pearson, 1897); in fact spurious correlation was the first troubling issue identified with compositional data. This phenomenon is best illustrated with the following example from Lovell et. al (2015), where they show how simply dividing two sets of random numbers (say abundances of OTU1 and OTU2), by a third set of random numbers (say abundances of OTU3) results in a strong correlation. Note that this phenomenon depends only on there being a common denominator.

```
n.obs <- 100
OTU.df <- data.frame(
    OTU1=rnorm(n.obs, mean=10, sd=1),
    OTU2=rnorm(n.obs, mean=10, sd=1),
    OTU3=rnorm(n.obs, mean=30, sd=4))
OTU.df <- transform(OTU.df,
    OTU1.over.OTU3= OTU1/OTU3,
    OTU2.over.OTU3= OTU2/OTU3)
plot(OTU.df$OTU1.over.OTU3,
    OTU.df$OTU2.over.OTU3, pch=19,
    cex=0.3,xlab="OTU1/OTU3",
    ylab="OTU2/OTU3")
```

Sub-compositions

Compositional data have the third property of a sub-composition incoherence of correlation metrics. That is, *correlations calculated on compositional datasets are unique to the particular dataset chosen* (Aitchison, 1986). This is problematic because high throughput sequencing experimental designs are *always* sub-compositions. Inspection of papers in the literature provide many examples. For example, in the 16S rRNA gene sequencing literature it is common practice to discard rare OTU

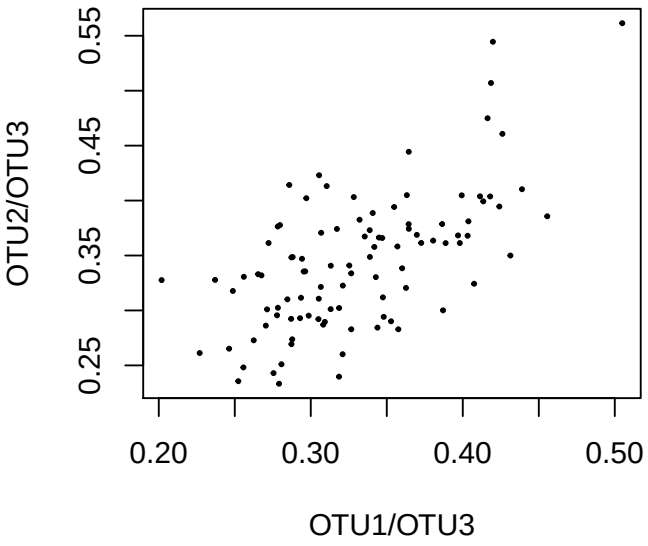

Figure 1: Spurious correlation in compositional data. Two random vectors drawn from a Normal distribution, were divided by a third vector also drawn at random from a Normal distribution. The two vectors have nothing in common, they should exhibit no correlation, and yet they exhibit a correlation coefficent of > 0.65 when divided by the third vector. See the introductory section of the Supplementary Information of Lovell (2015) for a more complete description of this phenomenon.

species prior to analysis and to re-normalize by dividing the counts for the remaining OTUs by the new sample sum. It is also common to use only one or a few taxonomic groupings to determine differences between experimental conditions. In the case of RNA-seq only the fraction of RNA of interest is sequenced, usually mRNA but other sub-fractions such as miRNA may be sequenced. All of these practices expose the investigator to the problem of non-coherence between sub-compositions. We must use compositionally-appropriate measures of correlation—more formally, we are attempting to find features that are compositionally associated. Compositional association is a more restricted measure of correlation and is explained more completely in the chapter on data transformations.

To summarize, compositional data has the following pathologies:

- The negative correlation bias means that any negative correlation observed in compositional data must be treated as suspect because it could arise simply because a different feature (or features) changed their abundance. There is currently no theoretically valid approach to identify true negative correlations in compositional data (Egozcue et al., 2018).
- The spurious correlation problem means that we can observe apparent postive correlations simply

by chance. I describe recent work that shows that spurious correlation is tractable.

- The sub-compositional incoherence of correlation is perhaps the most insidious property, but also the easiest to recognize. Here the correlation depends on the *exact* set of features present in the dataset. If the observed correlations change when the data are subset, then sub-compositional incoherence is in play.

Thus, one major reason to use compositional data methods is that you are more likely to report robust results, and the later practical chapters demonstrate the robustness of a compositional data analysis.

Practically speaking the negative correlation bias, the occurrence of spurious correlation, and the problem of sub-compositional incoherence means that *every microbial correlation network that has ever been published is suspect*, as is *every gene co-occurrence or co-expression network* unless compositionally appropriate compositional association metric was used (Erb and Notredame, 2016; Lovell et al., 2015; Quinn et al., 2017a). These approaches themselves have limitations and as originally constituted cannot deal with sparse data. However, recasting the data from count compositions to probability distributions allows these methods to be adapted to sparse data with some success (Bian et al.; Quinn et al., 2017a).

So can I analyze compositional data? How?

Much of the high throughput sequencing analysis literature seems to assume that data derived from high throughput sequencing are in some way unique, and that purpose-built tools must be used. However, there is nothing special about high-throughput sequencing data from the point of view of the analysis. Fortunately, the analysis of compositional datasets has a well-developed methodology (Pawlowsky-Glahn et al., 2015; Van den Boogaart and Tolosana-Delgado, 2013), much of which was worked out in the geological sciences.

Atichison (1986), Pawlsky-Glahn (2006), and Egozcue (2005), have done much work to develop rigorous approaches to analyze compositional data (Pawlowsky-Glahn and Buccianti, 2011). The essential step is to reduce the data to ratios between the D. This step does not move the data from the Simplex but does transform the data on the Simplex such that the distances between the ratios of the features are linear. The investigator must keep in mind that the distances are between ratios between features, not between counts of features (re-read this several times to wrap your head around it). Several transformations are in common use, but the one I believe is most applicable to HTS data is the centred log-ratio transformation or clr, where the data in each sample is transformed by taking the logarithm of the the ratio between the count value for each part and the geometric mean count: i.e., for D features in sample vector $\vec{\mathbf{X}} = [x_1, x_2, x_3, \dots x_D]$:

$$\vec{\mathbf{X}}_{clr} = [log(\frac{x_1}{gX}), log(\frac{x_2}{gX}) \dots log(\frac{x_D}{gX})] \quad (1)$$

where gX is the geometric mean of the features in sample $\vec{\mathbf{X}}$. The clr transformation is formally equivalent to a matrix of all possible pairwise ratios, but is a more tractable form. The clr transformation is not perfect by any means, but when there are large numbers of features the properties of the clr approach the ideal isometric log-ratio transformation or ilr. In the context of high throughput sequencing, where there are often hundreds or thousands of features the clr and the ilr have nearly indistinguishable properties.

The properties of the clr transformation are demonstrated in the chapter on data transformations.

Data transforms in high throughput sequencing

This chapter introduces data transformations that are prevalent in the ecological literature, and that have been extensively used in analyzing high throughput sequencing datasets. It is not intended to be a comprehensive analysis of data transformations, nor are all transformations described. In some cases, only one transformation is demonstrated when several transformations are obviously related. The `vegan` R package manual (Oksanen et al., 2017) has a very good description of many other data transformations and I recommend it to the interested reader: note that the `vegan` package is not compositionally appropriate.

This chapter is rather information dense, but the lessons in it are very important to understand the limitations of data analysis whenever the data are compositional. I have tried to make it easy and intuitive, but in the end you must work through the examples as best you can. All the source code needed to explore the data are included either directly here, or in an external file when the amount of code would break the flow of the narrative.

It is assumed that the output from a high-throughput sequencing experiment represents in some way the underlying abundance of the input DNA molecules. The input counts panels on the left side of Figure **??** shows two idealized experiments. The top left shows the case where the total count of all nucleic acid species in the input is constrained, the bottom left illustrates the case where the total count is unconstrained. These are modelled as a time series, but any process would produce the same results.

Constrained datasets occur if the increase or decrease in any component is exactly compensated by the increase or decrease of one or more others. Here the total count remains constant across all experimental conditions. Examples of constrained datasets would include allele frequencies at a locus where the total has to be 1, and the RNA-seq where the induction of genes occurs in a steady-state cell culture. In this case, any process, such as sequencing that generates a proportion simply recapitulates the data with sampling error. The unspoken assumption in most high throughput experimental designs is that this assumption is true— *it is not!*

An unconstrained dataset results if the total count is free to vary. Examples of unconstrained datasets would include ChIP-Seq, RNA-seq where we are examining two different conditions or cell populations, metagenomics, etc. Importantly, 16S rRNA gene sequencing analyses are almost always free to vary; that is, the total bacterial load is rarely constant in an environment. Thus, the unconstrained data type would be the predominant type of data that would be expected.

The relative abundance panels on the right side of Figure **??** shows the result of random sampling with a defined maximum value in these two types of datasets. This random sampling reflects the data that results from high throughput sequencing where the total number of reads is constrained by the instrument capacity. The data is represented as a proportion, but scales to parts per million or parts per billion without changing the shape. Here we see that the shape of the data after sequencing is very similar to the input data in the case of constrained, but is very different in the case of non-constrained data. In the unconstrained dataset, observe how the blue and red features appear to be constant over the first 10 time points, but then appear to decrease in abundance at later time points. Conversely, the black feature appears to increase linearly at early time points, but appears to become constant at late time points. Obviously, we would misinterpret what is happening if we compared early and late timepoints in the unconstrained dataset. It is also worth noting how the act of random sampling makes the proportional abundance of the rare OTU species uncertain in both the constrained and unconstrained data, but has little effect on the relative apparent effect on the relative abundance of OTUs with high counts.

Sequencing can change the shape of the data:

```
# the number of rare counts in the dataset
num.one = 100
ncol=num.one + 10

m.dub <- matrix(data=NA, nrow=20, ncol=ncol)
prop.m <- matrix(data=NA, nrow=20, ncol=ncol)
clr.m <- matrix(data=NA, nrow=20, ncol=ncol)

m.dub.u <- matrix(data=NA, nrow=20, ncol=ncol)
prop.m.u <- matrix(data=NA, nrow=20, ncol=ncol)
clr.m.u <- matrix(data=NA, nrow=20, ncol=ncol)

in.put <- c(10,20971,1,1,5,10,20,50,100,200,1000)

total.sum <- sum(in.put + 1) * 1000

# constrained with Gaussian noise
# one feature increases exponentially
# one feature decreases to compensate
for(i in 0:19){
    junk <- in.put * c(2^i,
        rep(1,num.one + 9))
    junk[3] <- total.sum - sum(junk)
    m.dub[i+1,] <- junk
```

```
    prop.m[i+1,] <- as.numeric(
        rdirichlet(1, junk) )
    clr.m[i+1,] <- log2(prop.m[i+1,])
        - mean(log2(prop.m[i+1,]))
}
# non-constrained with Gaussian noise
# same as above, without the decreasing
# feature
for(i in 0:19){
    junk <- in.put * c(2^i,
        rep(1,num.one + 9))
    m.dub.u[i+1,] <- junk
    prop.m.u[i+1,] <- as.numeric(
        rdirichlet(1, junk) )
    clr.m.u[i+1,] <- 2^(log2(prop.m.u[i+1,])
        - mean(log2(prop.m.u[i+1,])))
}

plot_c <- function(x, main, ylab, log=""){
    plot(x[,1], pch=20, type="b",  log=log,
    ylim=c(min(x), max(x)), xlab="time point",
    ylab=ylab)
    title( main=main, adj=0.5)
    points(x[,2], type="b",pch=21, col="gray")
    points(x[,3], type="b",pch=22, col="orange")
    points(x[,num.one + 10], type="b",
        pch=23, col="blue")
    points(x[,num.one+4], type="b", pch=24,
        col="red")
}

par(mfrow=c(2,4), mar=c(4,4,3,1) )

#constrained
plot_c(m.dub, main="Constrained\ncount",
    ylab="raw count")
plot_c(prop.m, main="Constrained\nproportion",
    ylab="raw proportion")
plot_c(m.dub, main="Constrained\ncount",
    ylab="log10 count", log="y")
plot_c(prop.m, main="Constrained\nproportion",
    ylab="log10 proportion", log="y")

# unconstrained
plot_c(m.dub.u, main="Unconstrained\ncount",
    ylab="raw count")
plot_c(prop.m.u, main="Unconstrained\nproportion",
    ylab="raw proportion")
plot_c(m.dub.u, main="Unconstrained\ncount",
     ylab="log10 count", log="y")
plot_c(prop.m.u, main="Unconstrained\nproportion",
     ylab="log10 proportion", log="y")
```

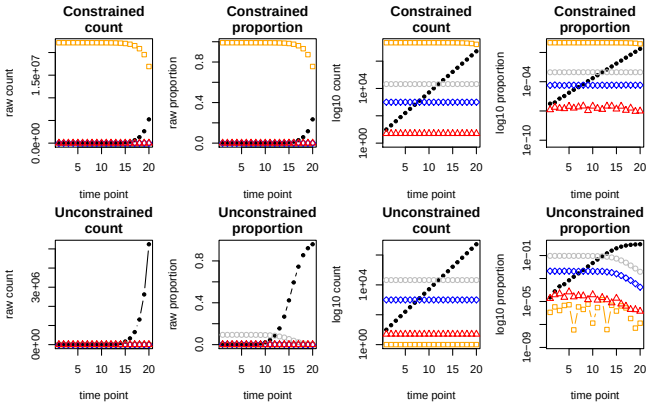

Figure 2: {fig-shape}High-throughput sequencing affects the shape of the data differently on constrained and unconstrained data. The two left panels show the absolute number of reads in the input tube for 20 steps where the green and black OTUs are changing abundance by 2-fold each step. The gray, blue and red OTUs are held at a constant number in each step in both cases. The second column shows the output in proportions (or ppm, or FPKM) after random sampling to a constant sum, as occurs on the sequencer. The orange OTU in the constrained data set is much more abundant than any other, and is changing to maintain a constant number of input molecules. Samples in the two right columns are the same values plotted on a log scale on the Y-axis for convenience. Note how the constrained data is the same before and after sequencing while the unconstrained data is severely distorted.

We assume that the abundance of each input DNA species that is observed after sequencing reflects a random sample of the input molecules. We can see that

that this may indeed be the case if the total number of molecules in the input sample is constant. This constraint would be met if, for example, an increase in one or more DNA species was balanced with an equivalent decrease in one or more different species. Such a constraint would be met In the figure, the red and blue OTU sequences are held constant in each sample, the green OTU is decreasing by 2 fold and the black OTU is increasing by 2 fold in each subsequent sample. The abundance of the orange OTU is adjusted such that the total sum of the OTU sequences in the input is held constant. Here it can be seen that the input counts and the relative abundance of each species following sequence have similar shapes, with the exception that the rarest species display significant variability because of random sampling.

Commonly used transformations are misleading

Current practice is to examine the datasets using 'relative abundance' values, that is, the proportional abundance of the OTUs either before or after normalization for read depth. This approach is equivalent to examining the input unconstrained data of the type seen in Figure **??** in the relative abundance sample space in the bottom right panel of the figure. This approach will obviously lead to incorrect assumptions in at least some cases. For example, depending upon the steps chosen to compare, the blue OTU, that has constant counts in the input, will be seen to either increase or decrease in abundance. Conversely, the green OTU, that is always decreasing in abundance will be seen to be constant if comparing samples 1-8.

The ecological literature offers many different transformations for such data, often as a way of making the data appear 'more normal'. Figure **??** shows the results of five such transformations.

- The frequency transform divides the each OTU value by the largest OTU count, and then divides the resulting values by the number of OTUs in the sample that had non-zero counts.
- The Hellinger transformation that takes the square root of the relative abundance (proportion) value.
- The range transform standardizes the values to have a range from 0 to 1. OTUs with 0 counts are set to 0.
- The standardize transform standardizes the values for each sample to have a mean of 0 and a variance of 1.
- The log transform divides each OTU count in a sample by the minimum non-zero count value, then takes the logarithm of the resulting value and adds 1. Counts of 0 are assigned a value of 0 to avoid taking the logarithm of 0.
- The centred log-ratio transformation divides the OTU values by the geometric mean OTU abundance, and then takes the logarithm.

It is obvious that the first four transformations result in data that badly mis-represents the shape of the actual input data. The log transformation, however results in the shape of the output data approximating the shape of the input data, except that the uncertainty of each data point is large. The ratio transform his transformation accurately recapitulates the shape of the original input data, and more accurately represents the uncertainty of each data point.

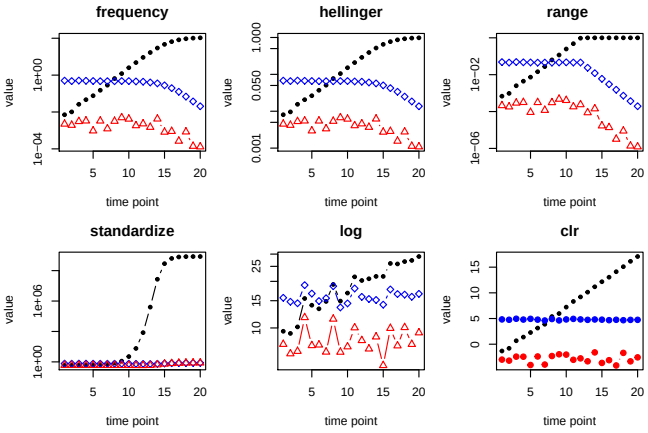

Figure 3: The effect of ecological transformations on unconstrained high throughput sequencing datasets. Data generated as in Figure **??** were transformed with five different approaches implemented in the vegan ecological analysis package, and with the entered log-ratio approach suggested by Aitchison.

Fundamentally, the goal of any experiment is to determine something about the environment that was sampled. After all, we are attempting to use HTS to determine something of interest about the underlying environment. Thus, we need to have some equivalence between the samples before sequencing and the samples after sequencing. The simplest case would be that there would be a linear relationship between the data that we could obtain from the environment, and the data that was actually collected by HTS.

We can think about the underlying data on a univariate basis; do the features across all samples follow a Gaussian distribution? or do they follow some unknown distribution? If so, can we transform the data to approximate a Gaussian distribution? This mode of thinking leads to the use of square-root, arcsine or Hellinger transformations since they appear to transform the data into

a distribution that can be interpreted. However, as we shall see below, none of these univariate transformations is suitable.

It is more desirable to think about HTS data in a multivariate way as a 'composition' because the total count of molecules in the underlying sample (the environment) is always a confounding variable (Lovén et al., 2012). This way of thinking led to multivariate data normalizations.

We will set up a random dataset, composed of four features (T, L, G, A) and 50 random samples with mean values of 100 tigers, 10000 ladybugs, 1000 gnus and 5 space aliens. The features will be drawn from a Normal distibution, although a random uniform distribution or any other distribution will give the same results. We are not, at this point, attempting to mimic a distribution found in a real dataset, but are instead showing the general properties of the distance metrics, and how those metrics compare when calculated on numerical data, obtained as counts in the environment, or on proportional data, obtained as relative abundances after sequencing.

```
set.seed(13)
T <- rnorm(50, mean=100, sd=25)
L <- rnorm(50, mean=10000, sd=2500)
G <- rnorm(50, mean=1000, sd=250)
A <- rnorm(50, mean=5, sd=2.5)
ran.dat <- cbind(T,L,G,A)
ran.dat[ran.dat <=0 ] <- 0.1

dist.ran.dat <- as.matrix(dist(
    ran.dat, method="euclidian"))

par(mfrow=c(1,3), pch=19, col=rgb(0,0,0,0.5),
    cex=1.5, cex.lab=1.5)

plot(T,L)
plot(L,G)
plot(G,A)
```

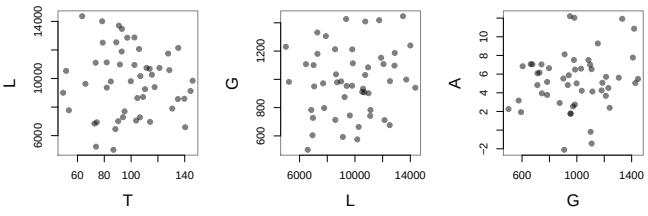

Figure 4: Plot of Ladybugs vs. Tigers, Gnus vs. Ladybugs and Aliens vs. Gnus for simulated random Normal data.

Figure 6 shows the relationships between three features in the actual dataset. We can see that the features are randomly normally distributed and uncorrelated in the scatter plots. Most tools attempt to infer something about this numerical dataset. For this to work, the data transforms must be linearly related in some way to this underlying data.

Let us see which, if any of the transforms fulfills this basic requirement.

Notation

We use the following notation throughout. Column vectors contain samples $\vec{\mathbf{s}}$ and row vectors contain features $\vec{\mathbf{f}}$. There are D features and n samples, thus the data are contained in matrix $M = D \times n$. The j^{th} sample is denoted as s_j, the i^{th} feature of all samples is denoted as s_{i-}, and the value for the i^{th} feature of the j^{th} sample is referred to as s_{ij}.

Simple proportional type transformations

The simplest normalization is to determine the relative abundance (rAB), or proportion, of the i^{th} feature in a sample as in Eq. 2. This normalization is also referred to as the total sum scaling (TSS) normalization.

$$rAB_i = \frac{s_i}{\sum \vec{\mathbf{s}}} \tag{2}$$

The rAB measure requires only the read count observed for a the feature s_i and the total read count of the sample $\sum \vec{\mathbf{s}}$. Since this measure is generally skewed, it is often log-transformed prior to analysis.

```
ran.dat.prop <- t(apply(ran.dat, 1,
    function(x) x/sum(x)))
par(mfrow=c(1,3), pch=19, col=rgb(0,0,0,0.5),
    cex=1.5, cex.lab=1.5)
plot(ran.dat.prop[,"T"],ran.dat.prop[,"L"],
    xlab="T.p", ylab="L.p")
plot(ran.dat.prop[,"L"],ran.dat.prop[,"G"],
    xlab="L.p", ylab="G.p")
plot(ran.dat.prop[,"G"],ran.dat.prop[,"A"],
    xlab="G.p", ylab="A.p")
```

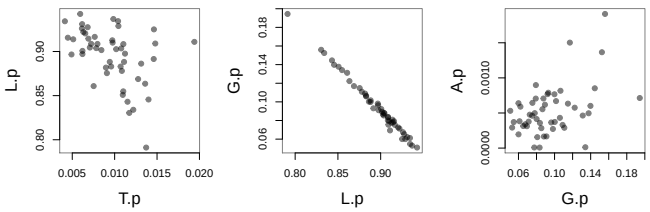

Figure 5: Plot of Ladybugs vs. Tigers, Gnus vs. Ladybugs and Aliens vs. Gnus for simulated random Normal data as proportions.

By comparing the proportions to the non-transformed data, we can see that the structure of the data itself has changed dramatically. The two most abundant features, G and L, which are uncorrelated in the actual data are now almost perfectly negatively correlated when the same data are converted and plotted as proportions, G.p vs L.p. This is because the data are now not real numbers, but are instead proportions and are constrained by the arbitrary sum of 1: *the data are now compositional data.*

A further normalization was proposed early in the RNA-seq field where the reads per kilobase per million mapped (RPKM)(Mortazavi et al., 2008) method was used initially to place the read counts for each feature within and between samples on a common scale.

For this we also needed to know a scaling factor K, and the length of the feature L_i; from this, the RPKM value for the i^{th} feature for each sample was calculated as in Eq. 3.

$$RPKM_i = \frac{K \cdot C_i}{\sum C \cdot L_i} \tag{3}$$

When the equation is placed in this form it is obvious that RPKM is simply a scaled rAB where each rAB value is divided by its length and multiplied by a constant. In compositional terms, RPKM is an unclosed perturbation of the original data; the data appear to be real numbers, but are actually proportions multiplied by a constant.

Further research suggested that RPKM was not appropriate for comparison of features between samples. The goal of RPKM was to 'count' reads per feature per cell. In the original paper the authors supplied an equivalence and an RPKM value of 1 RPKM equalled one transcript in each cell in the C2C12 cell line, but in liver cells, a value of 3 RPKM equalled one transcript per cell. Thus, from the start, this normalization was unable to normalize between-condition read counts.

The transcripts per million (TPM) normalization was advocated next (Li et al., 2010). Patcher (Pachter, 2011) showed the equivalence between RPKM and TPM, and in compositional terms TPM is simply a compositionally closed form of RPKM multiple by a constant as in Eq. 4.

$$TPM_i = \frac{RPKM_i}{\sum RPKM} \cdot K \tag{4}$$

The rAB, RPKM and TPM normalizations are thus all very similar, differing only in the scaling of individual features, and do not allow normalization between conditions unless the samples in the environment contain *exactly* the same input number of RNA molecules. In a very real sense, these normalizations deliver proportional data, scaled or perturbed to make the data appear as if they are numerical, and not proportional.

A related transformation is 'rarefaction' or subsampling without replacement to a defined per-sample read count. This transformation was widely used in the 16S rRNA gene sequencing field. Rarefaction to a common read count gives a composition, that is scaled such that low count features often are replaced by 0 values (McMurdie and Holmes, 2014). For this reason, rarefaction has now been largely replaced with the median of ratios method described below.

The median of ratios count normalization

Further work found that none of these methods were appropriate, since the read count per sample continued to confound the analyses (Lovén et al., 2012). Thus, the scaling normalization methods were proposed (Robinson and Oshlack, 2010). There are two main scaling normalizations, but both operate on the common assumption that by normalizing all counts in a sample to a per-sample midpoint value the normalization can impute the *number* of each feature in the environment. The approaches differ largely in how the midpoint is determined. The median of ratios method (MR) is instantiated in DESeq2 (and others), and the trimmed mean of M values (TMM) method is used by edgeR (and others). The DM method will be demonstrated and used, but the TMM gives substantially similar results, and uses the same basic logic since sample values are scaled by a per-sample feature-wise midpoint.

The DM method calculates the ratio of the features to the geometric mean, G_i, of each feature across all samples, and then takes as the normalization factor the median ratio per sample as the scaling factor. Each feature is then divided by the scaling factor to place each sample on an `equivalent' count scale. The idea is that the DM normalization`opens' the data from being compositional to being scaled counts. It is impossible to open the data, and while the scaled counts may have some useful properties, removing compositional constraints are not among them.

The multi-step normalization MR normalization attempts to normalize for sequencing depth thus 'opening' the data, and proceeeds as in the multistep Eq. 5. Here we start with two sample vectors $\vec{\mathbf{s}}_1$ and $\vec{\mathbf{s}}_2$, and calculate a vector of geometric means of the features $\vec{\mathbf{g}}$. Ratio vectors, $\vec{\mathbf{r}}_j$ are calculated by dividing the sample vectors by the geometric mean vector, and the median of the ratio vectors is determined. Finally, the sample vectors are divided by the median of the ratio vector for each sample.

$$\begin{aligned} \vec{\mathbf{g}} &= \mathrm{G}_{i-} \\ \vec{\mathbf{r}}_j &= \vec{\mathbf{s}}_j / \vec{\mathbf{g}} \\ \vec{\mathbf{d}}_j &= \vec{\mathbf{s}}_j / Md(\vec{\mathbf{r}}_j) \end{aligned} \tag{5}$$

In Table 1 we can see that the median ratio for each sample $\vec{\mathbf{r}}_j$ samples may be different in each sample, and that the particular feature that is the median may itself be different, the median feature is in boldface in the table. Thus, by construction the feature values in each sample can be scaled by different amounts in each sample.

Table 1: Example calculation of DM normalization

Feature	$\vec{\mathbf{s}}_1$	$\vec{\mathbf{s}}_2$	$\vec{\mathbf{g}}$	$\vec{\mathbf{r}}_1$	$\vec{\mathbf{r}}_2$	$\vec{\mathbf{d}}_1$	$\vec{\mathbf{d}}_2$
F1	1500	1000	1224.7	1.22	**0.81**	1219.5	1234.6
F2	25	15	19.4	1.29	0.77	20.3	18.5
F3	1000	500	707.1	1.41	0.71	813.0	617.3
F4	75	50	61.2	**1.23**	0.82	61.0	61.7
F5	500	1500	866.0	0.58	1.73	406.5	1851.9

```
ran.dat.DM <- t(des.norm(t(ran.dat.prop)))
par(mfrow=c(2,3), pch=19, col=rgb(0,0,0,0.5),
    cex=1.5, cex.lab=1.5)
plot(ran.dat.DM[,"T"],ran.dat.DM[,"L"],
    xlab="T.dm", ylab="L.dm")
plot(ran.dat.DM[,"L"],ran.dat.DM[,"G"],
    xlab="L.dm", ylab="G.dm")
plot(ran.dat.DM[,"G"],ran.dat.DM[,"A"],
    xlab="G.dm", ylab="A.dm")

plot(ran.dat[,"T"],ran.dat.DM[,"T"],
    xlab="T", ylab="T.dm")
plot(ran.dat[,"L"],ran.dat.DM[,"L"],
    xlab="L", ylab="L.dm")
plot(ran.dat[,"G"],ran.dat.DM[,"G"],
    xlab="G", ylab="G.dm")
```

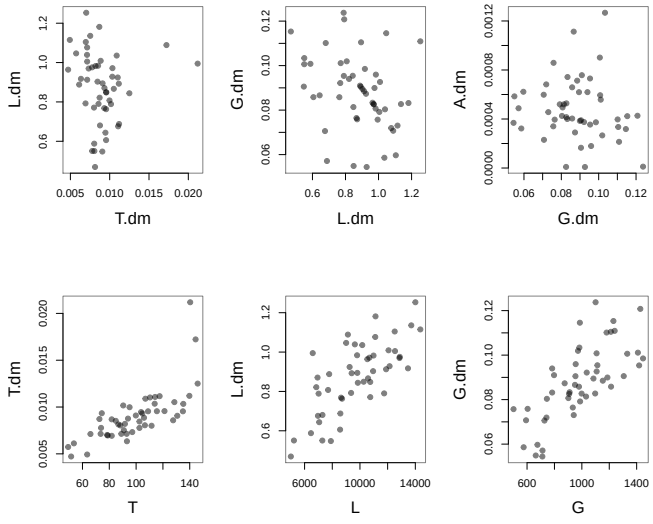

Figure 6: Plot of Ladybugs vs. Tigers, Gnus vs. Ladybugs and Aliens vs. Gnus for simulated random Normal data after the DM normalization (top row). Plot of input numerical and DM normalized data for Tigers, Ladybugs and Gnus (bottom row)

This DM transformation at first glance *appears* to fix the problem caused by converting the data from numbers to proportions. The pairs of points in the top row are no longer as strongly correlated and the data seem to be randomly distributed. However, plotting the actual numbers vs the DM transformed values shows that the DM transformation is not restoring the data to their original form, but to some other. In the absence of a solid theoretical foundation, it is difficult to say exactly how we should interpret these DM-transformed data. It should be pointed out that above plots were generated on the TSS-normalized dataset, however only the scale of the *dm* axes would change if the DM normalization was conducted on the original numerical data. Thus, conclusions derived from data that are DM-normalized actually tell us little about the underlying enviroment—despite the pervasive use of this transformation in the biomedical literature.

Log-ratio transformations

Aitchison (1986) introduced the concept of the log-ratio transformation.

There are three main log-ratio transformations; the additive log-ratio (alr), centred log-ratio (clr) and the isometric log-ratio (ilr) (Aitchison, 1986; Pawlowsky-Glahn et al., 2015).

Using the same notation as above for a sample vector $\vec{\mathbf{s}}$ of D 'counted' features (taxa, operational taxonomic units or OTUs, genes, etc.) $\vec{\mathbf{s}} = [s_1, s_2, ...s_D]$:

The alr is the simply the elements of the sample vector divided by a presumed invariant feature, which by convention here is the last one:

$$\vec{\mathbf{x}}_{alr} = [log(x_1/x_D), log(x_2/x_D), \ldots log(x_D - 1/x_D] \tag{6}$$

This is similar to the concept used in quantitative PCR, where the relative abundance of the feature of interest is divided by the relative abundance of a (presumed) constant 'housekeeping' feature. Of course there are two major drawbacks. First, that the experimentalist's knowledge of which, if any, features are invariant is necessarily incomplete. Second, is that the choice of the (presumed) invariant feature has a large effect on the result if the presumed invariant feature is not invariant, or if it is correlated with any other features in the dataset. Interestingly, an early proposal was to use the geometric mean of a number of internal controls (Vandesompele et al., 2002), leading to the next transformation.

The centered log-ratio (clr) transformation introduced by (Aitchison, 1983, 1986) uses the geometric mean of all features as the denominator:

$$\begin{aligned}\vec{\mathbf{x}}_{clr} =&[log(x_1/\mathrm{G}(\vec{\mathbf{x}})),\\ &log(x_2/\mathrm{G}(\vec{\mathbf{x}})),\\ &\ldots log(x_D/\mathrm{G}(\vec{\mathbf{x}}))]\end{aligned} \tag{7}$$

where $\mathrm{G}(\vec{\mathbf{x}}) = \sqrt[D]{x_1 \cdot x_2 \cdot ... \cdot x_D}$, the geometric mean of $\vec{\mathbf{x}}$.

The clr is often criticized since it has the property that the sum of the clr vector must equal 0. This constraint causes a singular covariance matrix; i.e., the sum of the covariance matrix is always a constant (Pawlowsky-Glahn et al., 2015). However the clr has the advantage of being readily interpretable, a value in the vector is its abundance *relative* to a mean value.

The ilr is the final transformation, and is a series of sequential log-ratios between two groups of features. For example, the philr transformation is the series of ratios between OTUs partitioned along the phylogenetic tree (Silverman et al., 2017), although any other sequential binary partitioning scheme is also possible (Pawlowsky-Glahn et al., 2015). The ilr transformation does not suffer the drawbacks of either the alr or clr, but does not allow for insights into relationships between single features in the dataset. Nevertheless, ilr transformations permit the full-range of multivariate tools to be used, and are recommended whenever possible.

The ilr and clr are directly comparable in a two important ways: First, the distances between samples computed using an ilr and clr transformation are equivalent. Second, the clr approaches the ilr in other respects as the number of features becomes large. In this respect, the large number of features—hundreds in the case of OTUs, thousands in the case of genes—in a typical experiment works in our favour. Thus, while not perfect, the clr is the most widely used transformation. However, care must be taken when interpreting its outputs since single features must always be interpreted as a ratio between the feature and the denominator used for the clr transformation. The problems of using clr are apparent when some subcomposition or group of taxa is analysed for further insight since the geometric mean of the subcomposition is not necessarily equal to that of the original composition, leading to potential inconsistencies.

Log-ratio values of any type do not need to be normalized since the total sum is a term in both the numerator and the denominator. Thus, the same log-ratio value will be obtained for the vector of raw read counts, or the vector of normalized read counts, or the vector of proportions calculated from the counts. Thus, log-ratios are said to be equivalence classes such that there is no information in the total count (aside from precision) (Barceló-Vidal et al., 2001).

Attempts to 'open' the data are doomed to failure because the data cannot be moved from the simplex to Euclidian space. The total count delivered by the sequencing instrument is a function of the instrument and not the number of molecules sampled from the environment, thus the total count has no geometric meaning. If the data are collected in such a way that the total count represents the actual count in the environment, then the data are not compositional and issues regarding compositional data disappear. However, at present all sequencing platforms deliver a fixed-sum, random sample of the proportion of molecules in the environment.

Note that this does not mean that the read depth is irrelevant since more reads for a sample translate into greater precision when estimating the proportions (Fernandes et al., 2013).

Comparing Transforms and Distances

The microbiome and transcriptome literature are replete with distance metrics, and it is common to find that a single study will use several distance metrics to report their findings. This is a problem since it shows that practitioners are unsure of the reason to use a metric, and the use of more than one metric leads to data dredging and research degrees of freedom—both of which increase the chances of finding false positives in the data to a surety.

Distance metrics can be broadly divided into those that require partitioning and those that do not. The UniFrac (Lozupone and Knight, 2005; Lozupone et al., 2011) and philr (Silverman et al., 2017) both require a phylogenetic tree, making these metrics applicable only to situations where the features can be so partitioned. For example, these distances are useful when examining 16S rRNA gene sequencing experiments. We have found that the unweighted UniFrac method is unreliable, and should be used with caution [Wong et al. (2016)}, a point that was made in the original UniFrac paper and subsequently forgotten. The philr metric is a drop-in replacement for the weighted UniFrac distance metric and should be used whenever possible, since `philr` is an ilr transformation of the data where the sequential binary partitions are made along the phylogenetic tree. The `philr` transformation is thus compositionally appropriate. In practice, the weighted UniFrac distance metric provides similar results to the Aitchison distance, described below, and the ilr distance calculated using the philr transform approaches the Aitchison distance when the number of features is large.

Several non-phylogenetic distances are in widespread use in the literature. These will be discussed in turn below, and their effects on distances between a random samples illustrated.

Distances in counts and proportion

Ideally, we use distance metrics to inform us as to something of relevance in the actual sample. That is, if we collect our data on the numbers of tigers, ladybugs, gnus and space aliens, what can we infer about the actual data *after sequencing*? which as we have seen, is the same as asking what can we infer after converting the data to relative abundances (proportions)?

There are two main ways to think about distances: Euclidian and Manhattan. The Euclidian distance is the straight-line distance between two points. If we have a rectangular room, the Euclidian distance between two corners would be the distance travelled by walking diagonally across the room from one corner to the other. The Manhattan distance would be the distance travelled by walking along the walls between the two corners. Obviously, the Manhattan distance will always be larger than the Euclidian distance. So how do these two simple metrics compare when calculate on numbers and on compositions?

```
library(vegan)

dist.ran.dat <- as.matrix(vegdist(
    ran.dat, method="euclidian"))
dist.ran.dat.MAN <- as.matrix(vegdist(
    ran.dat, method="manhattan"))
dist.ran.dat.prop <- as.matrix(vegdist(
    ran.dat.prop, method="euclidian"))
dist.ran.dat.prop.MAN <- as.matrix(vegdist(
    ran.dat.prop, method="manhattan"))

par(mfrow=c(2,2), pch=19, col=rgb(0,0,0,0.5),
    cex=1.5, cex.lab=1.5)

plot(dist.ran.dat[1,], dist.ran.dat.MAN[1,],
    xlab="Euclidian", ylab="Manhatten",
    main="Numbers")
plot(dist.ran.dat.prop[1,], dist.ran.dat.prop.MAN[1,],
    xlab="Euclidian.p", ylab="Manhattan.p",
    main="Proportions")
plot(dist.ran.dat[1,], dist.ran.dat.prop[1,],
    xlab="Euclidian", ylab="Euclidian.p",
    main="Number vs Proportions")
plot(dist.ran.dat.MAN[1,], dist.ran.dat.prop.MAN[1,],
    xlab="Manhattan", ylab="Manhattan.p",
    main="Number vs Proportions")
```

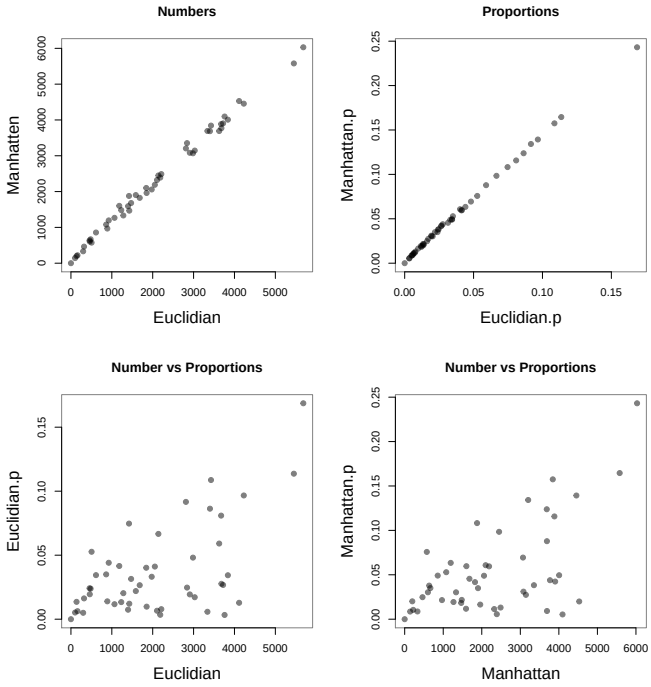

We can see that the Euclidian and Manhattan distances are generally correlated, but not identical, when comparing distances in the original set of random samples only, or when the data in the samples are converted to proportions. However, the distances between samples are very different when comparing the numerical and proportional data. This tells us that the inferences we make from sequencing data can not translate to inferences about the actual abundances of features in the environment, but only to their relative abundances. So which distance metric should we use for proportional data? It turns out that neither are suitable because these distance metrics assume linear differences between features, and this is not true in proportional data (Aitchison, 1986).

Data normalizations are often touted as removing the compositionality of the data. We shall see that this is not true, and inappropriate data transformations confound, rather than providing clarity.

Plotting three of the possible combinations, we can see that the features are essentially uncorrelated with each other and each sample is a random distances from any other. Any inference we make from transformations of this data must be relatable to this 'ground truth'. I now run through each of the transformations in turn, and illustrate the difference between the actual data, and the transformed data.

Bray-Curtis Dissimilarity

The Bray-Curtis dissimilarity is a Manhattan distance normalized to range between 0 and 1. In the test dataset, the Euclidian distance and the Bray-Curtis (BC) distances are essentially linearly related.

```
library(vegan)

dist.ran.dat.BC <- as.matrix(vegdist(
    ran.dat, method="bray"))
dist.ran.dat.MAN <- as.matrix(vegdist(
    ran.dat, method="manhattan"))
dist.ran.dat.DM.BC <- as.matrix(vegdist(
    ran.dat.DM, method="bray"))
dist.ran.dat.prop.BC <- as.matrix(vegdist(
    ran.dat.prop, method="bray"))

par(mfrow=c(2,2), pch=19, col=rgb(0,0,0,0.5),
    cex=1.5, cex.lab=1.5)

plot(dist.ran.dat.MAN[1,],dist.ran.dat[1,],
    xlab="S1 Euc", ylab="S1 BC",
    main="Euc vs BC")
plot(dist.ran.dat.BC[1,], dist.ran.dat.prop.BC[1,
    xlab="S1 BC", ylab="S1.p BC",
    main="BC vs BC.p")
plot(dist.ran.dat.BC[1,], dist.ran.dat.DM.BC[1,],
    xlab="S1 BC", ylab="S1.p DM",
    main="BC vs BC.DM")
plot(dist.ran.dat.prop.BC[1,], dist.ran.dat.DM.BC
    xlab="S1.p BC", ylab="S1.p DM",
    main="BC.p vs BC.DM")
```

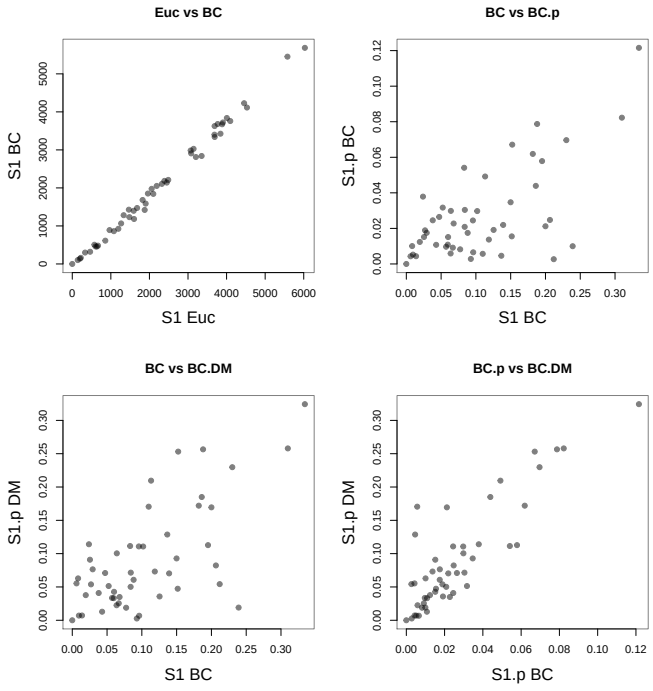

Euclidian Distance of TSS scaling transformation

The TSS scaling transformation is simply a conversion of each sample from a count to a proportion.

```
dist.ran.dat.prop <- as.matrix(dist(
    ran.dat.prop, method="euclidian"))
```

Euclidian Distance of DM transformation

The DM scaling transformation is a change in the scale of the sample vector $\vec{\mathbf{j}}$, where each sample is scaled by a different amount. This has the desirable property that it *can* restore the a conversion of each sample from a count to a proportion.

```
dist.ran.dat.DM <- as.matrix(dist(
    ran.dat.DM, method="euclidian"))

par(mfrow=c(2,2), pch=19, col=rgb(0,0,0,0.5),
    cex=1.5, cex.lab=1.5)

plot(ran.dat.DM[,"T"],ran.dat.DM[,"L"],
    xlab="T.dm", ylab="L.dm")
plot(ran.dat.DM[,"L"],ran.dat.DM[,"G"],
    xlab="L.dm", ylab="G.dm")
plot(ran.dat.DM[,"G"],ran.dat.DM[,"A"],
    xlab="G.dm", ylab="A.dm")
plot(dist.ran.dat[1,], dist.ran.dat.DM[1,],
    xlab="S1 vs all", ylab="S1.dm vs all.dm",
    main="Distance")
```

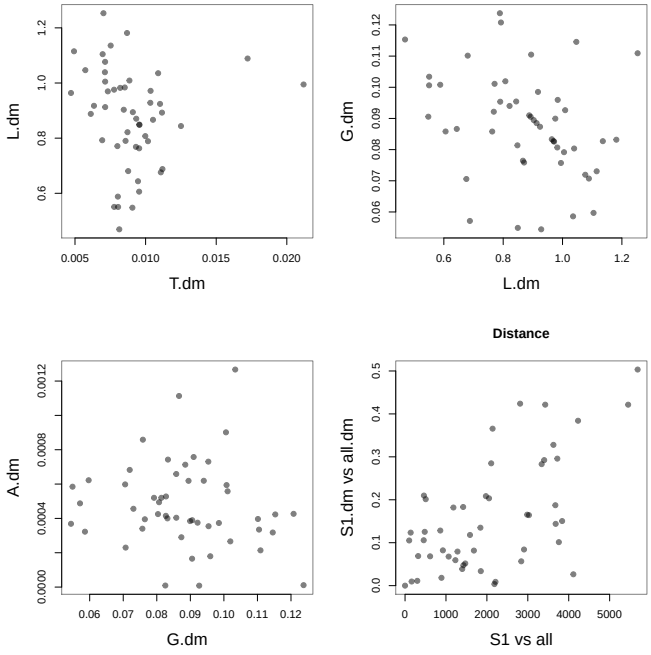


```
plot_ly(x=ran.dat[,"L"], y=ran.dat[,"T"],
z=ran.dat[,"G"])

plot_ly(x=ran.dat.prop[,"L"],
y=ran.dat.prop[,"T"], z=ran.dat.prop[,"G"])

plot_ly(x=ran.dat.DM[,"L"],
y=ran.dat.DM[,"T"], z=ran.dat.DM[,"G"])
```

Jensen-Shannon Divergence

Aitchison Distance

Exploring compositional data: the compositional biplot

There are three main data analysis issues that must be acknowledged.

First, the nature of these data are misunderstood. As outlined above, the number of counts observed per OTU are determined entirely by the capacity of the instrument and provide no information about the number of molecules in the input sample. Recall that both bacterial growth, and PCR are doubling processes and not linear processes, and so would be better modelled as $\log_2$ differences.

Understanding that we are dealing with fold-change data is an explicit acknowledgement that the data do not map to normal Euclidian space where differences are linear. Commonly used statistical tests expect linear differences between values and so are compromised to some degree, often catastrophically(Aitchison, 1986,vandenBoogaart2008320) Therefore, the often-used approaches of converting the OTU count values to proportions or percentages and conducting statistical tests on those values, or of using data reduction strategies such as Principle Component Analysis on the values are inappropriate because the differences between values are not linear. An alternative approach is to convert the OTU counts to ratios(Aitchison, 1986; Aitchison and J. Egozcue, 2005; Pawlowsky-Glahn and Buccianti, 2011; Pawlowsky-Glahn and Egozcue, 2006) which makes the differences between the ratios of values linear, and so allows the use of common statistical tests.

However the user must interpret the output as ratios between feature abundances rather than absolute differences(Pawlowsky-Glahn and Buccianti, 2011) This approach is described below.

Second, high throughput sequencing (HTS) data represent samples of an unknown underlying large number of molecules. Thus, there is a large and unappreciated error of estimation that is problematic when dealing with these data(Fernandes et al., 2013) The high error of estimation often results in false positive identification of differences, in fact, the statistical result can often be explained entirely by sampling variation. This error is not captured by rarefaction or even acknowledged by other normalization methods and should be estimated and accounted for when deciding what is a significant difference.

Third, 16S rRNA gene sequencing surveys, and similar experiments, contain many variables in each sample. Thus, any analysis that attempts to characterize the individual differences between groups must correct for the many hypotheses that are being tested. This step is often ignored, even in work published in very high profile journals subject to rigorous peer review.

The purpose of these notes is to show why HTS data for 16S rRNA gene sequencing, and any similar experiments such as RNA-seq, should be treated as ratio data and that it is possible to do so simply. We show that this approach accurately recapitulates the shape of the data for both constrained and unconstrained datasets. We show that converting the data to ratios can accurately model the very high variability at the low count margins, and that rarefaction under-estimates this variability. We use an example from the literature to show how ignoring these factors leads to improper conclusions.

References

Aitchison, J. (1983). Principal component analysis of compositional data. *Biometrika* 70, 57–65.

Aitchison, J. (1986). *The statistical analysis of compositional data*. London, England: Chapman & Hall.

Aitchison, J., and J. Egozcue, J. (2005). Compositional data analysis: Where are we and where should we be heading? *Mathematical Geology* 37, 829–850.

Andersson, A. F., Lindberg, M., Jakobsson, H., Bäckhed, F., Nyrén, P., and Engstrand, L. (2008). Comparative analysis of human gut microbiota by barcoded pyrosequencing. *PLoS One* 3, e2836. doi:10.1371/journal.pone.0002836.

Auer, P. L., and Doerge, R. W. (2011). A two-stage Poisson model for testing RNA-seq data. *Statistical applications in genetics and molecular biology* 10.

Barceló-Vidal, C., Martín-Fernández, J. A., and Pawlowsky-Glahn, V. (2001). "Mathematical foundations of compositional data analysis," in *Proceedings of IAMG*, 1–20.

Bian, G., Gloor, G. B., Gong, A., Jia, C., Zhang, W., Hu, J., et al. (). The gut microbiota of healthy aged chinese is similar to that of the healthy young. *mSphere* 2, e00327–17. doi:10.1128/mSphere.00327-17.

Egozcue, J. J., Pawlowsky-Glahn, V., and Gloor, G. B. (2018). Linear association in compositional data analysis. *Austrian Journal of Statistics* in press.

Egozcue, J., and Pawlowsky-Glahn, V. (2005). Groups of parts and their balances in compositional data analysis. *Mathematical Geology* 37, 795–828.

Erb, I., and Notredame, C. (2016). How should we measure proportionality on relative gene expression data? *Theory in Biosciences* 135, 21–36.

Erb, I., Quinn, T., Lovell, D., and Notredame, C. (2017). Differential proportionality - a normalization-free approach to differential gene expression. *bioRxiv*. doi:10.1101/134536.

Fernandes, A. D., Macklaim, J. M., Linn, T. G., Reid, G., and Gloor, G. B. (2013). ANOVA-like differential expression (aLDEx) analysis for mixed population rNA-seq. *PLoS One* 8, e67019. doi:10.1371/journal.pone.0067019.

Fernandes, A. D., Reid, J. N., Macklaim, J. M., McMurrough, T. A., Edgell, D. R., and Gloor, G. B. (2014). Unifying the analysis of high-throughput sequencing datasets: Characterizing RNA-seq, 16S rRNA gene sequencing and selective growth experiments by compositional data analysis. *Microbiome* 2, 15.1–15.13. doi:10.1186/2049-2618-2-15.

Friedman, J., and Alm, E. J. (2012). Inferring correlation networks from genomic survey data. *PLoS Comput Biol* 8, e1002687. doi:10.1371/journal.pcbi.1002687.

Gloor, G. B., and Reid, G. (2016). Compositional analysis: A valid approach to analyze microbiome high-throughput sequencing data. *Can J Microbiol* 62, 692–703. doi:10.1139/cjm-2015-0821.

Gloor, G. B., Hummelen, R., Macklaim, J. M., Dickson, R. J., Fernandes, A. D., MacPhee, R., et al. (2010). Microbiome profiling by Illumina sequencing of combinatorial sequence-tagged PCR products. *PLoS One* 5, e15406. doi:10.1371/journal.pone.0015406.

Gloor, G. B., Macklaim, J. M., Vu, M., and Fernandes, A. D. (2016a). Compositional uncertainty should not be ignored in high-throughput sequencing data analysis. *Austrian Journal of Statistics* 45, 73–87. doi:doi:10.17713/ajs.v45i4.122.

Gloor, G. B., Wu, J. R., Pawlowsky-Glahn, V., and Egozcue, J. J. (2016b). It's all relative: Analyzing microbiome data as compositions. *Ann Epidemiol* 26, 322–9. doi:10.1016/j.annepidem.2016.03.003.

Gorzelak, M. A., Gill, S. K., Tasnim, N., Ahmadi-Vand, Z., Jay, M., and Gibson, D. L. (2015). Methods for improving human gut microbiome data by reducing variability through sample processing and storage of stool. *PLoS One* 10, e0134802. doi:10.1371/journal.pone.0134802.

Hawinkel, S., Mattiello, F., Bijnens, L., and Thas, O. (2017). A broken promise: Microbiome differential abundance methods do not control the false discovery rate. *Briefings in Bioinformatics*, bbx104.

Horner-Devine, M. C., Lage, M., Hughes, J. B., and Bohannan, B. J. M. (2004). A taxa-area relationship for bacteria. *Nature* 432, 750–3. doi:10.1038/nature03073.

Hsiao, E. Y., McBride, S. W., Hsien, S., Sharon, G., Hyde, E. R., McCue, T., et al. (2013). Microbiota modulate behavioral and physiological abnormalities associated with neurodevelopmental disorders. *Cell* 155, 1451–63. doi:10.1016/j.cell.2013.11.024.

Kaul, A., Mandal, S., Davidov, O., and Peddada, S. D. (2017). Analysis of microbiome data in the presence of excess zeros. *Front Microbiol* 8, 2114. doi:10.3389/fmicb.2017.02114.

Kurtz, Z. D., Müller, C. L., Miraldi, E. R., Littman, D. R., Blaser, M. J., and Bonneau, R. A. (2015). Sparse and compositionally robust inference of microbial ecological networks. *PLoS Comput Biol* 11, e1004226. doi:10.1371/journal.pcbi.1004226.

Li, B., Ruotti, V., Stewart, R. M., Thomson, J. A., and Dewey, C. N. (2010). RNA-seq gene expression estimation with read mapping uncertainty. *Bioinformatics* 26, 493–500. doi:10.1093/bioinformatics/btp692.

Lovell, D., Pawlowsky-Glahn, V., Egozcue, J. J., Marguerat, S., and Bähler, J. (2015). Proportionality: A valid alternative to correlation for relative data. *PLoS Comput Biol* 11, e1004075. doi:10.1371/journal.pcbi.1004075.

Lovén, J., Orlando, D. A., Sigova, A. A., Lin, C. Y., Rahl, P. B., Burge, C. B., et al. (2012). Revisiting global gene expression analysis. *Cell* 151, 476–82. doi:10.1016/j.cell.2012.10.012.

Lozupone, C., and Knight, R. (2005). UniFrac: A new phylogenetic method for comparing microbial communities. *Applied and environmental microbiology* 71, 8228–8235.

Lozupone, C., Lladser, M. E., Knights, D., Stombaugh, J., and Knight, R. (2011). UniFrac: An effective distance metric for microbial community comparison. *ISME J* 5, 169–72. doi:10.1038/ismej.2010.133.

Mandal, S., Van Treuren, W., White, R. A., Eggesbø, M., Knight, R., and Peddada, S. D. (2015). Analysis of composition of microbiomes: A novel method for studying microbial composition. *Microb Ecol Health Dis* 26, 27663.

Martín-Fernández, J., Barceló-Vidal, C., Pawlowsky-Glahn, V., Buccianti, A., Nardi, G., and Potenza, R. (1998). Measures of difference for compositional data and hierarchical clustering methods. in *Proceedings of IAMG*, 526–531.

McMurdie, P. J., and Holmes, S. (2014). Waste not, want not: Why rarefying microbiome data is inadmissible. *PLoS Comput Biol* 10, e1003531. doi:10.1371/journal.pcbi.1003531.

Mortazavi, A., Williams, B. A., McCue, K., Schaeffer, L., and Wold, B. (2008). Mapping and quantifying mammalian transcriptomes by RNA-seq. *Nat Methods* 5, 621–8. doi:10.1038/nmeth.1226.

Oksanen, J., Blanchet, F. G., Friendly, M., Kindt, R., Legendre, P., McGlinn, D., et al. (2017). Vegan: Community ecology package. Available at: https://CRAN.R-project.org/package=vegan [Accessed].

Pachter, L. (2011). Models for transcript quantiffication from RNA-seq. *ArXiv* 1104.3889.

Parameswaran, P., Jalili, R., Tao, L., Shokralla, S., Gharizadeh, B., Ronaghi, M., et al. (2007). A pyrosequencing-tailored nucleotide barcode design unveils opportunities for large-scale sample multiplexing. *Nucleic Acids Res* 35, e130. doi:10.1093/nar/gkm760.

Paulson, J. N., Stine, O. C., Bravo, H. C., and Pop, M. (2013). Differential abundance analysis for microbial marker-gene surveys. *Nat Methods* 10, 1200–2. doi:10.1038/nmeth.2658.

Pawlowsky-Glahn, V., and Buccianti, A. (2011). *Compositional data analysis: Theory and applications*. John Wiley & Sons.

Pawlowsky-Glahn, V., and Egozcue, J. J. (2006). Compositional data and their analysis: An introduction. *Geological Society, London, Special Publications* 264, 1–10. doi:10.1144/GSL.SP.2006.264.01.01.

Pawlowsky-Glahn, V., Egozcue, J. J., and Tolosana-Delgado, R. (2015). *Modeling and analysis of compositional data*. John Wiley & Sons.

Pearson, K. (1897). Mathematical contributions to the theory of evolution. – on a form of spurious correlation which may arise when indices are used in the measurement of organs. *Proceedings of the Royal Society of London* 60, 489–498.

Quinn, T. P., Erb, I., Richardson, M. F., and Crowley, T. M. (2017a). Understanding sequencing data as compositions: An outlook and review. *bioRxiv*. doi:10.1101/206425.

Quinn, T., Richardson, M. F., Lovell, D., and Crowley, T. (2017b). Propr: An R-package for identifying proportionally abundant features using compositional data analysis. *bioRxiv*. doi:10.1101/104935.

Robinson, M. D., and Oshlack, A. (2010). A scaling normalization method for differential expression analysis of RNA-seq data. *Genome Biol* 11, R25.1–R25.9. doi:10.1186/gb-2010-11-3-r25.

Robinson, M. D., McCarthy, D. J., and Smyth, G. K. (2010). EdgeR: A bioconductor package for differential expression analysis of digital gene expression data. *Bioinformatics* 26, 139–40. doi:10.1093/bioinformatics/btp616.

Silverman, J. D., Washburne, A. D., Mukherjee, S., and David, L. A. (2017). A phylogenetic transform enhances analysis of compositional microbiota data. *Elife* 6, 21887. doi:10.7554/eLife.21887.

Thorsen, J., Brejnrod, A., Mortensen, M., Rasmussen, M. A., Stokholm, J., Al-Soud, W. A., et al. (2016). Large-scale benchmarking reveals false discoveries and count transformation sensitivity in 16S rRNA gene amplicon data analysis methods used in microbiome studies. *Microbiome* 4, 62. doi:10.1186/s40168-016-0208-8.

Tsilimigras, M. C. B., and Fodor, A. A. (2016). Compositional data analysis of the microbiome: Fundamentals, tools, and challenges. *Ann Epidemiol* 26, 330–5. doi:10.1016/j.annepidem.2016.03.002.

Van den Boogaart, K. G., and Tolosana-Delgado, R. (2013). *Analyzing compositional data with r*. Springer, London, UK.

Vandesompele, J., De Preter, K., Pattyn, F., Poppe, B., Van Roy, N., De Paepe, A., et al. (2002). Accurate

normalization of real-time quantitative rT-pCR data by geometric averaging of multiple internal control genes. *Genome Biol* 3, RESEARCH0034.

Washburne, A. D., Silverman, J. D., Leff, J. W., Bennett, D. J., Darcy, J. L., Mukherjee, S., et al. (2017). Phylogenetic factorization of compositional data yields lineage-level associations in microbiome datasets. *PeerJ* 5, e2969. doi:10.7717/peerj.2969.

Weiss, S., Xu, Z. Z., Peddada, S., Amir, A., Bittinger, K., Gonzalez, A., et al. (2017). Normalization and microbial differential abundance strategies depend upon data characteristics. *Microbiome* 5, 27. doi:10.1186/s40168-017-0237-y.

Wong, R. G., Wu, J. R., and Gloor, G. B. (2016). Expanding the UniFrac toolbox. *PLoS One* 11, e0161196. doi:10.1371/journal.pone.0161196.